

Ultrafast Photoionization and Energy Absorption in Bulk Silicon and Germanium

Tzveta Apostolova^{1,2}

¹Institute for Nuclear Research and Nuclear Energy,
Bulgarian Academy of Sciences

²Institute for Advanced Physical Studies,
New Bulgarian University
Sofia, Bulgaria
e-mail: tzveta@innrne.bas.bg

Boyan Obreshkov

Institute for Nuclear Research and Nuclear Energy,
Bulgarian Academy of Sciences

Sofia, Bulgaria
e-mail: obreshko@innrne.bas.bg

Abstract— Intense femtosecond laser pulses are routinely used to stimulate ultrafast transformations in the properties of the dielectric materials. Understanding the connection of the microscopic response with the macroscopic properties of the photoexcited material, requires application of space and time resolved experimental techniques and development of predictive theoretical tools to rationalize experimental data. In the field of modeling ultrashort laser-matter interactions, progress has been achieved in understanding photoionization and atomic scale properties of ultrafast electronic currents within the Time Dependent Density Functional Theory. However, first-principles approaches for description of micro- and macroscopic material responses are usually limited to ultrashort time scales of order 10fs, since the calculation is time consuming and requires large computational resources. We overcome this limitation by applying the empirical pseudopotential method for describing the electronic properties of dielectric materials. The deposited energy, photoelectron densities, ultrafast currents and optical breakdown thresholds in bulk silicon and germanium, irradiated by intense 30 fs pulsed laser with near-infrared and mid-infrared wavelengths (800nm-5 μ m) and intensities 1GW/cm²-1TW/cm² are obtained by solving the time-dependent Schrodinger equation in single active electron approximation.

Keywords- group IV semiconductors; femtosecond laser irradiation; nonthermal melting; nonlinear optical properties; multiphoton and tunnel ionization.

I. INTRODUCTION

Femtosecond laser irradiation is suitable for studying fundamental processes in solids, such as ultrafast chemical reactions and phase transitions. Photoionization and photoexcitation of electrons in solids is the predominant mechanism of laser-pulse energy deposition, which subsequently may induce ultrafast transformation of the material. Depending on the laser parameters (wavelength, polarization, pulse energy and pulse duration), transformations of solid-state properties may be reversible or irreversible. Intense laser field may strongly distort the electronic structure by transiently converting insulators and dielectrics into metallic state on a sub femtosecond scale [1]. This distortion results in optical-field-induced transient and reversible currents below the bulk damage threshold [2]. For

sufficiently strong laser fields close to the bulk damage threshold, irreversible transformation occurs resulting in non-thermal melting [3], sublimation and ablation on a longer time scale. When intense ultrashort laser pulse is used for material modification, the different stages during the phase transformation can be studied using time-resolved techniques. Study of the nonthermal melting of germanium using ultrafast x-ray diffraction techniques was reported and it was assumed that this ultrafast process takes place when ~10% of the valence-band electrons are excited to the conduction band [4]. The ultrafast phase transitions and the dynamics of melting, ablation and re-solidification of germanium surfaces was studied [5] using space- and time-resolved measurements of the surface reflectivity.

At the same time, femtosecond laser interaction of semiconductors has found important practical applications, e.g. the graphitization of diamond bulk and creation of color centers could be used in quantum information processing and the manipulation of qubits [6]. Laser-induced graphitization in bulk diamond is used in the design of particle detectors [7]. Dielectric surfaces can be promptly converted into plasmonic state by ultrafast laser irradiation, supporting propagation of surface plasmon-polaritons. For instance, the plasmonic properties of silicon and germanium can be used for metamaterial applications at near-infrared and mid-infrared wavelengths [8][9].

Ultrafast phase transformation of semiconductors under intense femtosecond irradiation starts with photoionization and deposition of laser energy onto the electrons. In this paper, we study the nonlinear response of silicon and germanium irradiated by intense near-IR and mid-IR laser pulses with time duration of 30 femtoseconds. For this purpose, we have developed numerical methods for integration of the time-dependent Schrodinger equation in single active electron approximation [10]-[13].

More specifically, we estimate optical breakdown thresholds of silicon and germanium from the deposited laser energy inside the bulk. We find two regimes of absorption: at lower intensities, the absorbed energy depends sensitively on the laser wavelength due to multiphoton transitions, and a crossover occurs at higher intensity, when absorption becomes wavelength-independent. The merging point in laser intensity is material specific. In the multi-photon absorption regime, the dependence of the absorbed energy on the driving laser intensity is determined and scaling laws are obtained. For mid-IR wavelengths, we find that a smaller

number of photons is required to cross the direct bandgap as compared to the minimum number of photons allowed by energy conservation. For near-IR wavelengths, the scaling law exhibits a perturbative trend for both materials. At high intensity, the absorbed energy is wavelength independent and scales linearly with the laser intensity. This paper is organized as follows: Section II presents material and laser specific parameters which are inputs for the numerical solution of Time Dependent Schrodinger Equation. The numerical results for the photoelectron density and absorbed energy are discussed in section II A. The time evolution of the laser energy transfer to electrons, their number density and the ultrafast macroscopic currents are discussed in Section II B. Our main conclusions are included in Section III.

II. NUMERICAL RESULTS AND DISCUSSION

A. Photoelectron density and absorbed energy

The photon energies corresponding to the four wavelengths used in the calculations are: 1.55 eV (800 nm), 1.24 eV (1 μm) for near-IR irradiation, and 0.41 eV (3 μm), 0.248 eV (5 μm) for the mid-IR laser. The band-structures of Si and Ge were obtained numerically using the empirical pseudo-potential method [14]. The corresponding bulk lattice constants and selected transition energies between valence and conduction band states in the Brillouin zone are shown in Table 1. The calculated threshold for indirect electronic excitations in Ge is 0.9 eV and it is 0.8 eV for Si. In long wavelength approximation, the laser pulse ionizes electrons through the direct band gaps, the threshold for direct transitions in Ge is 1.2 eV and the corresponding threshold in Si is 3.4 eV.

TABLE I. BULK LATTICE CONSTANTS AND SELECTED BANDGAP ENERGIES IN GERMANIUM AND SILICON

	Lattice constant [Å]	$\Gamma_{25'}-\Gamma_{2'}$ [eV]	$\Gamma_{25'}-\Gamma_{15}$ [eV]	$\Gamma_{25'}-L_1$ [eV]	$\Gamma_{25'}-X(\Delta_1)$ [eV]
Ge	5.66	1.2	3.4	0.9	1.0
Si	5.43	3.9	3.4	1.8	0.8

In Fig. 1 and Fig. 2 we show the number of conduction electrons N_e produced by photoionization of silicon and germanium as a function of laser intensity after the irradiation with near-IR pulse of wavelength 800 nm. The number of photoelectrons in silicon increases monotonously with the increase of the laser intensity and follows a perturbative trend $N_e \sim I^2$ due to two-photon transition across the minimal direct bandgap. At the highest intensity shown (1.0 TW/cm^2), $N_e = 0.08$. For the same laser wavelength, similar results are found using the Time Dependent Density Functional Theory and the number of photoelectrons per atom at 1.0 TW/cm^2 obtained by the authors is $N_e = 0.06$ [15].

The intensity dependence of the number of photoelectrons in germanium, shown in Fig. 2, exhibits the same trend $N_e \sim I^2$ due to above threshold ionization via two photon transition from the light hole to the conduction band

involving Bloch crystal momentum displaced from the Brillouin zone center. When the laser peak intensity reaches 0.1 TW/cm^2 we find a change of slope in the photoionization yield following linear trend with $N_e \sim I$. At the highest intensity shown (1.0 TW/cm^2) the number of conduction electrons per atom is $N_e = 0.07$.

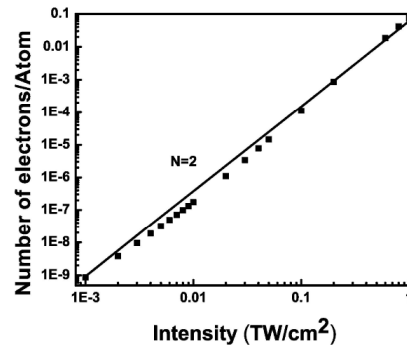


Figure 1. Intensity dependence of the number of conduction electrons per atom in bulk Si after the irradiation with 30fs near infrared pulse with wavelength 800 nm. The laser is linearly polarized along the [111] direction.

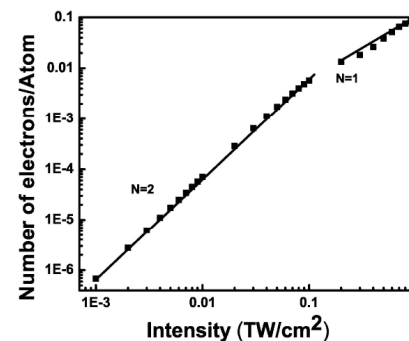


Figure 2. Intensity dependence of the number of conduction electrons per atom in bulk Ge after the irradiation with 30fs near infrared pulse with wavelength 800 nm. The laser is linearly polarized along the [111] direction.

Fig. 3 and Fig. 4 show the intensity dependence of the energy transferred to electrons in bulk Ge and Si after the irradiation with near-IR and mid-IR pulses. We distinguish two regimes of electronic excitation based on the scaling of the absorbed energy with the laser intensity. In the high-intensity regime the absorbed energy becomes independent of the laser wavelength above material-specific threshold intensity - 0.5 TW/cm^2 for Ge, and 1.0 TW/cm^2 for Si. The absorbed energy per Ge atom is 0.2 eV at threshold intensity, and is 0.28 eV per Si atom. Both absorbed energies at threshold are above the melting temperatures of the two materials - 0.104 eV (1211 Kelvin) for Ge and 0.145 eV (1687 Kelvin) for Si, respectively [16]. In this high intensity regime we find that the ultrafast energy deposition inside the bulk is sufficient to cause nonthermal melting. The low-intensity regime is wavelength dependent and is characterized by a superlinear scaling of the absorbed energy as a function of the intensity $\Delta E \sim I^N$. When $N = N_{\text{min}}$, where N_{min} is the minimum number of photons required to bridge

the direct band gap, perturbative multiphoton absorption is expected.

Fig. 3 shows the intensity dependence of the deposited laser energy in Ge. In the low-intensity regime, we obtain $N=2$ for irradiation with 800 nm wavelength, while resonant one-photon absorption is expected with $N_{\min}=1$. For the 1 μm wavelength, the same trend is observed for laser intensities below 5 GW/cm^2 . In the high intensity regime, the absorbed energy scales linearly with the laser intensity. For irradiation with mid-IR pulse having a 3 μm wavelength, we find $N=1$ for intensities up to 3 GW/cm^2 , which is less than the minimal number of photons required to cross the direct bandgap $N_{\min}=2$, however $N=N_{\min}=2$ in the range from 3 GW/cm^2 up to the threshold intensity for Ge. For 5 μm wavelength, in the range below 2 GW/cm^2 , $N=1$, for intensities 2 GW/cm^2 - 8 GW/cm^2 , $N=N_{\min}=4$, and $N=2$ for laser intensities above 15 GW/cm^2 .

Fig. 4 shows the intensity dependence of the deposited laser energy in silicon. In the low-intensity regime and in the near-IR region for the 800 nm wavelength, we find perturbative trend in the whole intensity range with $N_{\min}=N=2$, corresponding to two-photon absorption process, while for the 1 μm wavelength, three-photon transition occurs with $N=N_{\min}=3$ for all intensities considered. For irradiation with Si with mid-IR laser, we find that there is a threshold intensity 10 GW/cm^2 below which no laser energy is absorbed into the material. For the 3 μm wavelength, and laser intensity above this threshold, the absorbed energy exhibits the superlinear trend with $N=6$, which is less than the minimum number of photons required to cross the direct bandgap ($N_{\min}=8$). For 5 μm wavelength, a similar trend is observed: there is a step-like increase of the absorbed energy with $N=7$ and strong deviation from perturbative trend with $N_{\min}=13$. It is worth noting that for irradiation with 30 fs mid-IR laser pulses, the pulse length is a small multiple of an optical cycle. In this regime the tunnel ionization of electrons is expected to become dominant mechanism.

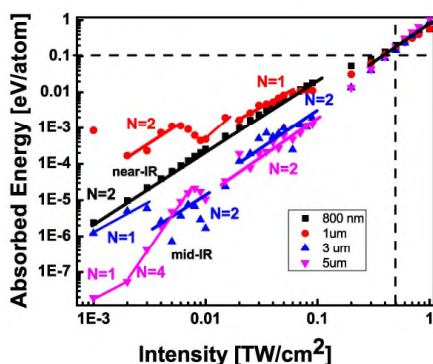


Figure 3. Intensity dependence of the energy absorbed per atom in bulk Ge irradiated by 30 fs laser pulse with laser wavelengths - (square) 800 nm, (circle) 1 μm , (triangle) 3 μm and (inverted triangle) 5 μm . The laser pulses are linearly polarized along the [111] direction. The horizontal dashed line indicates the energy corresponding to the melting temperature of the material and the vertical dashed line designates the position of the threshold intensity above which the deposited energy is wavelength independent.

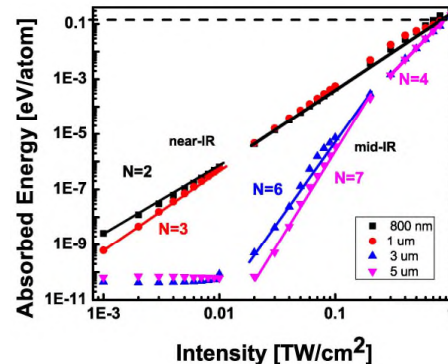


Figure 4. Intensity dependence of the energy absorbed per atom in bulk Si irradiated by 30 fs laser pulse with laser wavelengths - (square) 800 nm, (circle) 1 μm , (triangle) 3 μm and (inverted triangle) 5 μm . The laser pulses are linearly polarized along the [111] direction. The horizontal dashed line indicates the energy corresponding to the melting temperature of the material and the vertical dashed line specifies the position of the threshold intensity above which the deposited energy is wavelength independent.

B. Transient number density, absorbed energy and ultrafast macroscopic currents

The ultrafast laser energy deposition and the typical electron dynamics in the bulk of the two photoexcited materials is shown in Fig.5 - Fig.8 for two cases of different laser intensities, 0.05 TW/cm^2 and 0.6 TW/cm^2 . Fig. 5 (a) shows the transient electron densities in Ge for peak laser intensity 0.05 TW/cm^2 , corresponding to the four different wavelengths discussed in Sec. II A. The photoelectron density displays transient oscillations due to non-linear response of electrons, associated with the generation of intense second harmonic. The amplitude of these transient density oscillations increases substantially when the laser wavelength increases from near-IR to mid-IR region. Charge-carrier generation occurs on the rising edge of the pulse and competes with recombination of electron-hole pairs after the pulse peak to determine the final photoionization yield. A hot electron-hole plasma with number density of around 10^{20} cm^{-3} (near-IR wavelengths) and below 10^{19} cm^{-3} (mid-IR wavelengths) is established after the end of the pulse. Fig. 5 (b) shows the temporal evolution of the absorbed energy in bulk Ge after irradiation with peak laser intensity 0.05 TW/cm^2 . The absorbed energy displays oscillatory behavior dependent on the laser wavelength. For irradiation with near-IR laser, energy is efficiently transferred to the electronic system on the rising edge of the pulse. For irradiation with mid-IR wavelengths, large-amplitude transient fluctuations of the energy are exhibited during the pulse, but no significant amount of energy is transferred to electrons after the end of the

pulse.

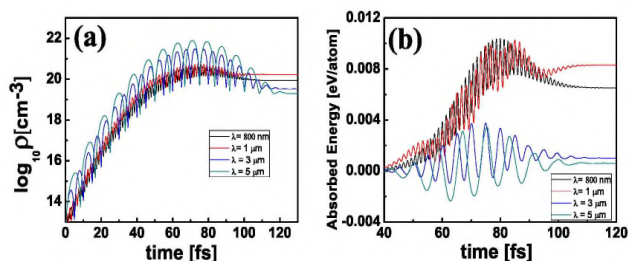


Figure 5. Transient electron density (a) and absorbed energy per atom (b) in bulk Ge irradiated by laser pulses of different wavelengths (indicated in the legend). The laser pulses are linearly polarized along the [111] direction and their peak intensity is 0.05 TW/cm².

For the higher intensity 0.6 TW/cm², shown in Fig. 6, the transient fluctuations of the absorbed energy are strongly suppressed during the irradiation with near-infrared pulse (cf. Fig. 6 (b)), however large amplitude of the oscillations is still prominent for mid-infrared wavelengths, particularly for the 5 μm wavelength. The deposited laser energy after the end of the pulse is wavelength independent. A similar trend is exhibited in the number density: regardless on the laser wavelength, an electron-hole plasma with number density of 10²¹ cm⁻³ is established after the pulse peak, cf. Fig. 6 (a).

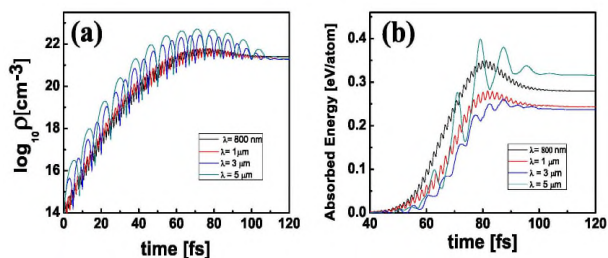


Figure 6. Transient electron density (a) and absorbed energy per atom (b) in bulk Ge irradiated by laser pulses of different wavelengths (indicated in the legend). The laser pulses are linearly polarized along the [111] direction and their peak intensity is 0.6 TW/cm².

Fig. 7 (a-b) shows the temporal evolution of the absorbed energy and photoelectron density in bulk Si for peak laser intensity 0.05 TW/cm², corresponding to the four different wavelengths discussed in Sec. IIA. Similar to the case of photoexcited Ge, laser induced oscillatory dynamics of electrons is exhibited. The amplitude of the transient energy fluctuations is large for all four wavelengths during the pulse. The absorbed energy after the end of the pulse is highly inefficient for both near infrared and mid-infrared wavelength regimes as seen in Fig. 7 (b). For near-IR wavelengths, the density of electron-hole pairs at the pulse peak is 10²⁰ cm⁻³, and this number density is reduced with two orders of magnitude to 10¹⁸ cm⁻³ after the end of the pulse as shown in Fig. 7 (a). For mid-IR laser, the

fluctuation in the number of conduction electrons is strongly enhanced during the irradiation: the density of electron-hole pairs at the pulse peak reaches 10²² cm⁻³. The virtual population of the conduction band disappears after the pulse peak and the number density of the generated real charge carriers is substantially reduced below 10¹⁵ cm⁻³.

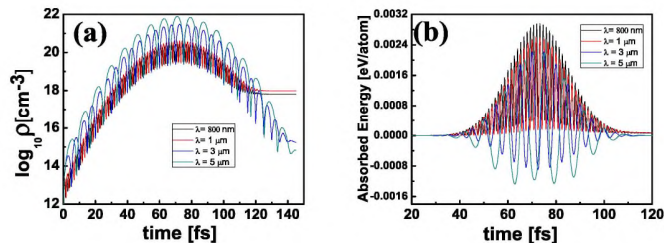


Figure 7. Transient electron density (a) and absorbed energy per atom (b) in bulk Si irradiated by laser pulses of different wavelengths (indicated in the legend). The laser pulses are linearly polarized along the [111] direction and their peak intensity is 0.05 TW/cm².

For the higher intensity 0.6 TW/cm², shown in Fig. 8 (a-b), the transient oscillations in energy are reduced for near infrared wavelengths and energy is efficiently absorbed after the end of the pulse as seen in Fig. 8 (b). The comparison between Fig. 6 (b) and Fig. 8 (b), shows that energy is much less efficiently absorbed in Si as compared to Ge for the same laser irradiation conditions. This is reasonable in view of the much larger direct bandgap in Si. Energy absorption is less efficient for 1 μm compared to 800 nm. For 5 μm, the transient fluctuations of the energy overshoot during the pulse with very high amplitude, indicating very efficient transient energy transfer to electrons. After the end of the pulse, energy absorption in bulk Si is 4 times more efficient for near-infrared wavelengths than for the mid-infrared ones. The density of the hot electron-hole plasma is around 10²⁰ cm⁻³ (for near-IR wavelengths) and is around 10¹⁹ cm⁻³ (for mid-IR wavelengths) as shown in Fig. 8 (a).

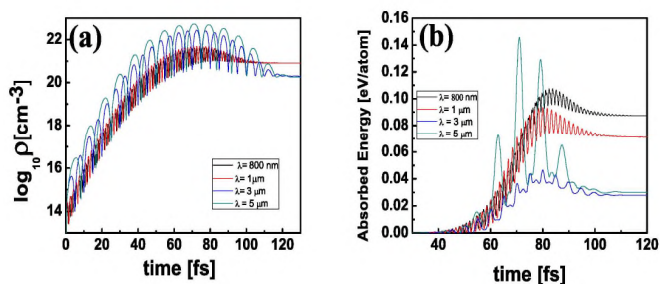


Figure 8. Transient electron density (a) and absorbed energy per atom (b) in bulk Si irradiated by laser pulses of different wavelengths (indicated in the legend). The laser pulses are linearly polarized along the [111] direction and their peak intensity is 0.6 TW/cm².

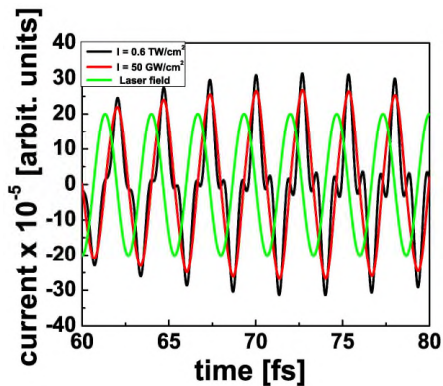


Figure 9. Induced electric currents in bulk Si for two intensities 0.05 TW/cm² (red) and 0.6 TW/cm² (black) and the applied laser field with wavelength 800 nm.

Fig. 9 shows the time evolution of the laser induced macroscopic currents inside the bulk Si during the irradiation with near-IR pulse of wavelength 800nm: two electric current waveforms, corresponding to the low and high laser intensity regimes - 50 GW/cm² and 0.6 TW/cm² are plotted, and the temporal profile of the driving laser field is shown. At the lower intensity of 50 GW/cm², the induced electric current lags behind the driving electric field by $\pi/2$, which indicates linear response of silicon. For that reason, energy transfer to electrons is unlikely, because negligible amount of work is done on the electron system by the driving laser field during each half-cycle. At the higher laser intensity - 0.6 TW/cm², the current still lags behind by nearly $\pi/2$ relative to the driving field, but the transient current develops a rapid subcycle structure due to nonlinear response of the electrons. As a consequence an efficient transfer of laser energy to the electrons occurs during each half cycle, the cumulative effect of these sub-cycle energy transfers eventually results in dielectric breakdown.

III. CONCLUSIONS AND FUTURE WORK

We have presented theoretical/numerical results of photo-excitation and energy absorption in Ge and Si, irradiated with intense, ultrashort laser pulses of 30 fs, using time-dependent Schrodinger equation in single active electron approximation. We obtained the wavelength and laser intensity dependence of the absorbed energy in the bulk of the materials. After the irradiation with near-infrared pulses of relatively low intensity, the intensity dependence of the electronic excitation energy exhibits perturbative trends due to multiphoton absorption process. Tunnel ionization of electrons is the relevant photoionization mechanism induced by strong few-cycle, mid-infrared pulses. For Si irradiated by mid-infrared laser pulse, we find that there is a laser intensity threshold below which no energy is absorbed inside the bulk; no such response is found for Ge. In the high laser intensity regime, we find intensity thresholds above which the absorbed energy per atom becomes independent of the laser

wavelength. In this regime, the electronic excitation energies exceed the melting temperatures in Si and Ge, which is a prerequisite for nonthermal melting of the materials. Below the bulk damage threshold, the results may provide valuable information for ultrafast changes of optical constants of silicon and germanium at near- and mid-infrared frequencies. Above the estimated dielectric breakdown thresholds, our numerical results may be helpful in finding a regime of laser parameters relevant for the nonthermal laser processing of silicon and germanium. In a follow up paper we intend to present results on the detailed microscopic response of electrons in these materials, including the transient density distributions and interband coherences.

ACKNOWLEDGMENT

This work is supported by the Bulgarian National Science Fund under Contracts No. DNTS/France-01/9, No.DN-18/7 and No.DN-18/11 (T.A.) and by the Bulgarian National Science Fund under Contract No. 08-17 (B.O.).

REFERENCES

- [1] G. Wachter, C. Lemell, J. Burgdorfer, S. A. Sato, X. Tong, and K. Yabana, "Ab Initio Simulation of Electrical Currents Induced by Ultrafast Laser Excitation of Dielectric Materials", *Phys. Rev. Lett.*, vol. 113, pp. 087401-087406, 2014, doi:10.1103/PhysRevLett.113.087401.61.2643
- [2] A. Schiffrin, T. Paasch-Colberg, N. Karpowicz, V. Apalkov, D. Gerster, S. Muhlbrandt, et al., *Nature* vol. 493, pp. 70-74, 2013, doi: 10.1038/nature11567
- [3] A. Rousse, C. Rischel, S. Fourmaux, I. Uschmann, S. Sebban, G. Grillon, P. Balcou, et al., "Non-thermal melting in semiconductors measured at femtosecond resolution", *Nature*, vol. 410, pp. 65-68, 2001
- [4] K. Sokolowski-Tinten and D. von der Linde, "Generation of dense electron-hole plasmas in silicon", *Phys. Rev. B* vol. 61, pp. 2643-2650, 2000, doi:10.1103/PhysRevB.61.2643
- [5] J. Bonse, G. Bachelier, J. Siegel, and J. Solis, "Time- and space-resolved dynamics of melting, ablation, and solidification phenomena induced by femtosecond laser pulses in germanium", *Physical Review B*, vol. 74, pp. 134106-134119, 2006, doi: 10.1103/PhysRevB.74.134106
- [6] J. Forneris, S. Ditalia Tchernij, P. Traina, E. Moreva, N. Skukan, M. Jakširc, et al., "Mapping the Local Spatial Charge in Defective Diamond by Means of N-V Sensors—A Self-Diagnostic Concept", *Physical Review Applied* vol. 10, pp. 014024-014039, 2018
- [7] S. Lagomarsino, M. Bellini, C. Corsi, S. Fanetti, F. Gorelli, Liontos, G. Parrini, et al., "Electrical and Raman-imaging characterization of laser-made electrodes for 3D diamond detectors", *Diamond Relat. Mater.* vol. 43, pp. 23-28, 2014, doi:10.1016/j.diamond.2014.01.002
- [8] A. Boltasseva and H. A. Atwater, *Science* vol. 331, pp. 290-291, 2011, doi: 10.1126/science.1198258
- [9] I. Staude and J. Schilling, "Metamaterial-inspired silicon nanophotonics", *Nature Photonics*, vol. 11, pp. 274-284, 2017
- [10] B. Obreshkov and T. Apostolova, "Photoionization of Diamond Interacting with Intense 30fs Laser Pulse", *Bulg. J. Phys.* vol. 42, pp. 305-314, 2015
- [11] S. Lagomarsino, S. Sciortino, B. Obreshkov, T. Apostolova, C. Corsi, M. Bellini, et al., "Photoionization of monocrystalline CVD diamond irradiated with ultrashort intense laser pulse", *Phys. Rev. B*, vol. 93, pp. 085128-085139, 2016, doi: 10.1103/PhysRevB.93.085128

- [12] T. Apostolova, B. Obreshkov, Ionin A.A., Kudryashov S.I., Makarov S.V., Mel'nik N.N., et al., "Ultrafast photoionization and excitation of surface-plasmon-polaritons on diamond surfaces", *Applied Surface Science*, vol. 427, pp. 334-343, 2018, doi:10.1016/j.apsusc.2017.07.263
- [13] T. Apostolova and B. Obreshkov, "High harmonic Generation from Bulk Diamond driven by Intense femtosecond laser pulse", *Diamond and Related Materials*, vol. 82, pp. 165-172, 2018, doi: 10.1016/j.diamond.2017.12.013
- [14] M. L. Cohen and T. K. Bergstresser, *Phys. Rev.* vol. 141, pp. 789-796, 1966
- [15] S. A. Sato, K. Yabana, Y. Shinohara, T. Otobe, and G. F. Bertsch, "Numerical pump-probe experiments of laser-excited silicon in nonequilibrium phase", *Phys. Rev. B*, vol. 89, pp. 064304- 064312, 2014, doi: 10.1103/PhysRevB.89.064304
- [16] C. C. Yang and Q. Jiang, "Effect of pressure on melting temperature of silicon and germanium", *Materials Science Forum*, Vols. 475-479 (2005), pp. 1893-1896, doi:10.4028/www.scientific.net/MSF.475-479.1893